JOURNAL OF GEOPHYSICAL RESEARCH, VOL. 101, NO. C4, PAGES 8943–8956, APRIL 15, 1996

Extraction of tidal streams from a ship-borne acoustic Doppler current profiler using a statistical-dynamical model

Michael Dowd and Keith R. Thompson

Department of Oceanography, Dalhousie University, Halifax, N.S., Canada

Abstract. We present a method for extracting the barotropic tide directly from the time-space series of horizontal velocity obtained by a ship-borne acoustic Doppler current profiler (ADCP). The method is conceptually straightforward, easy to implement, and suitable for operational use. It involves fitting a limited area tidal model, based on the linearized depth-averaged shallow water equations, to the ADCP record. The flows across the open boundaries of the model domain are assumed periodic in time with known frequencies corresponding to the tidal constituents of interest. The unknown tidal amplitudes and phases at the boundary are estimated from interior ADCP velocities using an inverse method; the solution of the shallow water equations is posed as a boundary value problem in the frequency domain, and the estimation procedure is based on generalized least squares regression. Results obtained include tidal maps, a tidal residual series, and associated error estimates. An application of the method to ship ADCP data collected on a cruise to the Western Bank region of the Scotian Shelf off the east coast of Canada is described. The tidal estimates and the residual field obtained are verified by comparison to other data collected during the cruise. The residual circulation shows an anticyclonic gyre centered on the crest of Western Bank and a northward current to the west of this region.

1. Introduction

The ship mounted acoustic Doppler current profiler (ADCP) has become an important instrument for the study of coastal and continental shelf circulation. It has been used for such purposes as measuring flow around headlands [*Geyer and Signell*, 1990], identifying internal wave structure [*Marmorino and Trump*, 1992], determining the flow in a channel [*Simpson et al.*, 1990], and as an independent check on numerical models [*Howarth and Proctor*, 1992]. The basic measurement is a vertical profile of the horizontal current obtained at regular time intervals along the cruise track of the ship. The flexibility of a moving observation platform allows for diverse sampling strategies and full areal coverage of many circulation features.

Ready interpretation of ship-borne ADCP data in coastal and continental shelf regions is confounded by the presence of tides in the record. For a current time series from a fixed location, harmonic analysis [e.g., *Godin*, 1972] is often used to remove the tides. However, for the ADCP record, the movement of the ship precludes any such straightforward procedure. In such a case, tide removal must take into account not only the periodic variation through time but also the spatially varying amplitude and phase resulting from the progression of the tide through the region.

A number of methods have been proposed for removing tides from ADCP records. The simplest involves designing the sampling strategy so that repeat measurements are made at fixed locations at regular time intervals. Conventional harmonic analysis can then be used for de-tiding the series [*Geyer and Signell*, 1990; *Simpson et al.*, 1990]. This method is not always feasible because sampling is often dictated by other considerations. Another method uses prior estimates of the tides from observations or numerical modeling which allows the tidal signal to be removed directly from the ADCP record [*Howarth and Proctor*, 1992, *Foreman and Freeland*, 1991]. Clearly, this approach is restricted to areas in which the tides are well known. A final method fits arbitrary basis functions to the ADCP record to describe the spatially varying tidal amplitude and phase [*Candela et al.*, 1992]. The use of these interpolation functions, which ignore the dynamics, can be problematic in regions with relatively complicated flow fields [*Foreman and Freeland*, 1991].

The problem of tide extraction can be readily considered in the context of oceanographic data assimilation. *Bennett and McIntosh* [1982] first treated open-ocean tidal modeling as an inverse problem. Their approach was based on the variational analysis of fixed tide gauge

Paper number 95JC02693.
0148-0227/96/95JC-02693$05.00

and current meter time series using a shallow water model as a weak constraint. More recently, sea level and current meter time series have been analyzed with a tidal model, enforced as a strong constraint, for the purpose of estimating various model parameters [*Das and Lardner*, 1991, *Lardner et al.*, 1993] and boundary conditions [*Lardner*, 1993]. This paper addresses the problem of tidal analysis of a time-space series of velocity (a ship-borne ADCP record) using simple tidal dynamics.

We consider the problem of tide extraction from the ADCP record as a discrete inverse problem. Our proposed method is straightforward, robust, and computationally efficient. These qualities make it suitable for operational shipboard use. The focus is on limited area models with one or more open boundaries and spatial scales of 10 to 1000 km. Tidal flows across the open boundaries of the model are treated as unknown quantities and estimated from ADCP data in the interior. In this manner, tidal maps over the model domain are obtained directly from the ADCP data. These can then be used for a more detailed examination of the subtidal circulation.

The paper is organized as follows. Section 2 describes the Western Bank region of the Scotian Shelf off Canada's east coast and presents current meter and ship-borne ADCP data collected on the cruise of April 1992. Tidal dynamics and the tidal model are then introduced in section 3. Section 4 sets up the problem of tidal analysis of ADCP data as a regression problem in the frequency domain. Finally, application of these methods to the ADCP data collected on Western Bank is carried out in section 5. A summary and discussion follow in section 6.

Note that, for notational clarity, and a succinct explanation of the tidal extraction method, complex arithmetic and a number of matrix equations are introduced in sections 3 and 4. Implementation of the method may be facilitated by recasting the problem in terms of real-valued quantities. Furthermore, the computational burden may be reduced by calculating some matrix products directly and taking advantage of matrix partitioning where it exists.

2. Observations

As part of the Ocean Production Enhancement Network's (OPEN) cod recruitment study, a number of cruises have been made recently to the Western Bank region of the Scotian Shelf off Canada's east coast. Figure 1 shows the bathymetry of this region and details the study area of the April 1992 cruise. The physics of the Scotian Shelf are relatively complex, particularly for the outer shelf which interacts strongly with the open ocean (for a review, see *Smith and Schwing* [1991]). For the Western Bank region the Rossby number is of order 0.1, and a hydrographic survey taken during the cruise (conductivity-temperature-depth (CTD) stations shown in Figure 1) indicated that this region is generally well mixed in the vertical down to about 70 m. Some density structure becomes evident below this level and along the edge of the Bank [*Griffin and Lochmann*, 1992]. Density profiles collected on the cruise are used, in section 5, for checking the de-tided ADCP currents.

Current data were obtained on the April 1992 cruise from three current meters deployed at the locations shown in Figure 1 and at the depths given in Table 1. Time series plots of horizontal velocity are given in Figure 2. Density and velocity profiles suggest that the measured currents reflect the depth-mean flow. The tidal signal associated with the M_2, S_2, K_1 and O_1 constituents was extracted from each of the current meter time series. (In section 5, these are compared with the ADCP results). Table 1 indicates that the tides in this region account for approximately 75% of the total variance in the current meter records.

The wind-driven component of the de-tided current meter series was isolated by expressing it as a linear combination of the wind vector (shown in Figure 2) at lags 0, 16, 32, and 48 hours. (A complex, least-squares regression was used to determine the coefficients). This implies a slab-like response of the water column to wind forcing, which is reasonable provided that the current meter is far from coastal boundaries and the Ekman depth is less than the total water depth [*Pollard and Millard*, 1970]. In fact, analysis of the transfer function between the wind and the three current time series indicates a flow roughly to the right of the wind with a damped resonant response centered on the inertial frequency, consistent with simple Ekman dynamics. Table 1 indicates the nontidal variance is roughly equally split between the wind and a residual associated with low-frequency (subsynoptic) variability.

Ship-borne ADCP data were also available for the cruise period. The original ADCP data consisted of a time-space series of vertical profiles of the horizontal current, bottom referenced and output every 3 minutes. Since the focus here is on extracting the barotropic tide, the vertical profiles were depth averaged from the surface to 60m (or bottom) and sampled at 15 minute time intervals. The end result is a pair of horizontal velocity components each with a corresponding observation time and location.

A time series representation of the ADCP data is shown in Figure 3. The time series plots show strong diurnal and semidiurnal oscillations, and power spectra of the data confirm that most of the energy is contained in these bands. The spring-neap cycle is evident in the overall amplitude of the tide; however, complex demodulation of the series suggests that the amplitude and phase of the tide vary within the individual tidal frequencies. One fairly extreme example of this occurs at approximately 240 hours when irregularities in the velocity signal are found with the movement of the ship over the shelf break.

To represent the spatial dimension of the ADCP data, Figure 4 shows vectors of hourly ADCP data for various time windows during the cruise period. Clearly, the data are difficult to interpret in this case. The rotary nature of the current vector in the presence of

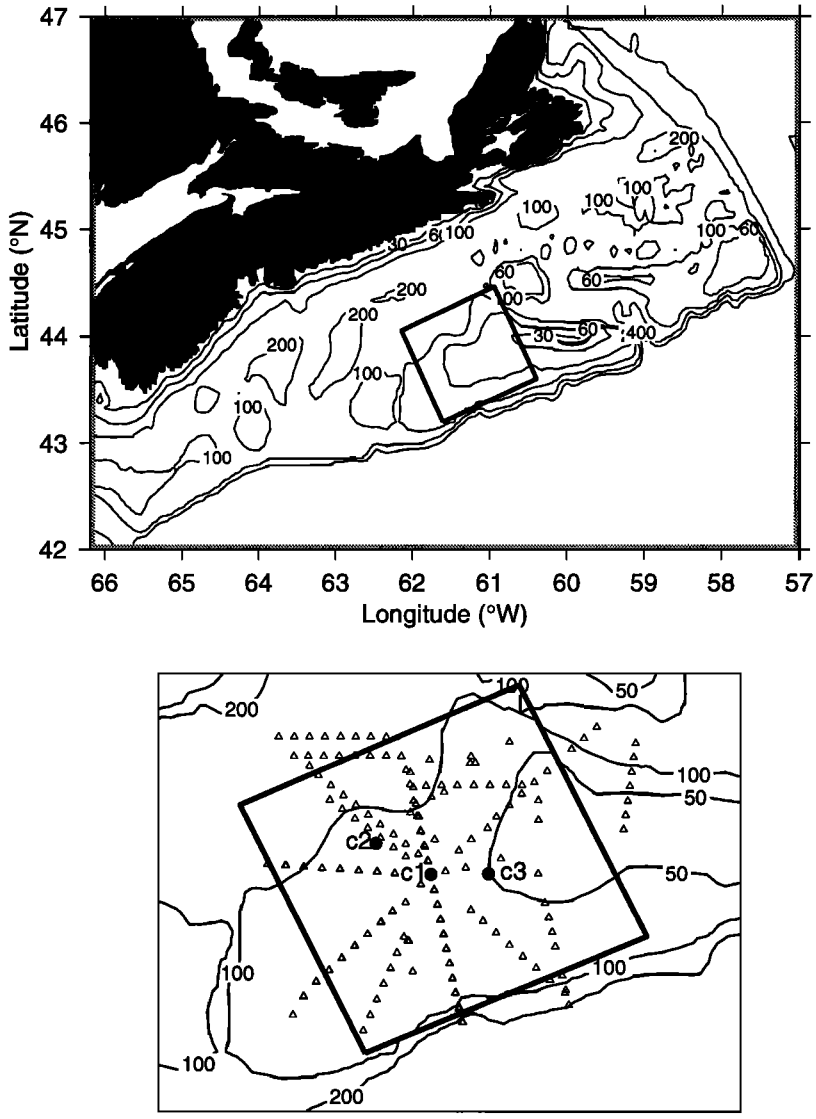

Figure 1. (Upper panel) Coastline of Nova Scotia and the bathymetry, in meters, of the Scotian Shelf. The rectangular box indicates the study region, and model domain, on Western Bank. (Lower panel) Detail of the boxed region in the upper panel with locations of the three current meters (c1, c2, c3, represented by solid dots) deployed on the April 1992 cruise. CTD stations from this cruise are also shown (triangles).

tides suggests a number of apparent convergences and divergences in the current field. A meaningful residual circulation can only be obtained by careful removal of the tides from the record.

3. Tidal Model

A model describing the spatial and temporal variation of the barotropic tide is an integral part of our tidal extraction procedure. A suitable model for the Western Bank region is based on the linearized, depth-averaged shallow water equations

$$\frac{\partial \vec{u}}{\partial t} + f\vec{k} \times \vec{u} + g\nabla\eta + \frac{\lambda}{h}\vec{u} = \vec{0}$$
$$\frac{\partial \eta}{\partial t} + \nabla \cdot (\vec{u}h) = 0 \qquad (1)$$

where t is time, $\vec{u}(\vec{x},t)$ contains the horizontal components of the depth-averaged current, and $\eta(\vec{x},t)$ represents the sea surface elevation above some undisturbed depth of water $h(\vec{x})$. The horizontal gradient operator is denoted $\nabla = (\partial/\partial x, \partial/\partial y)$. The Coriolis parameter is represented by f, and $\vec{k}$ is the unit vertical vector. The remaining parameters are the acceleration of gravity g and the bottom friction coefficient λ. For simplicity, a linear friction based on the depth-averaged velocity is used.

Denoting the flow normal to the boundary by $\vec{u} \cdot \vec{n}$, where $\vec{n}$ is the unit outward normal at the boundary of the domain, we postulate open boundary flows of the form

$$\vec{u} \cdot \vec{n} = \sum_{k=1}^{K} \Re\{a_k e^{i\omega_k t}\}. \qquad (2)$$

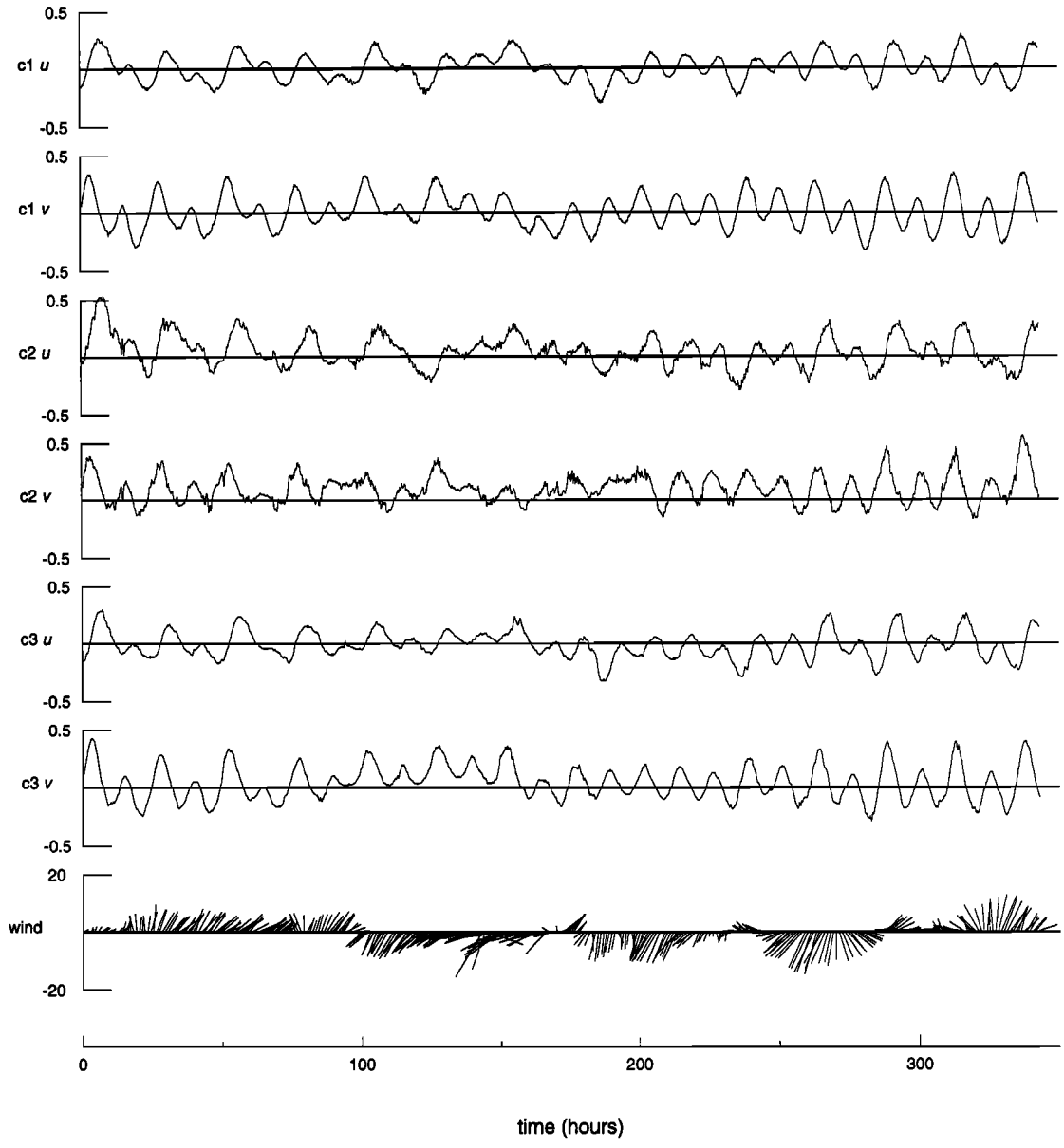

Figure 2. Time series plots of the east-west u and north-south v velocity components for the three current meters (c1, c2, c3, in $\mathrm{m\,s^{-1}}$). The time series of the wind vector (in $\mathrm{m\,s^{-1}}$) is also shown in the bottom panel. The series begins at 2115, April 20, 1992.

Here, ω_k is the frequency of the kth tidal constituent, a_k is its complex amplitude, $\Re$ denotes the real part of a complex quantity, and the summation is over the K tidal constituents of interest. Although the tidal frequencies are well known, the boundary amplitudes ($|a_k|$) and phases (arg a_k) constitute a major source of uncertainty.

The flows across the open boundary for each tidal constituent are parameterized in terms of spatial structure functions. For a north-south oriented boundary, the spatial variation in the complex amplitude a_k of the normal velocity at the boundary is expressed as

$$a_k(y) = h^{-1} \sum_{r=1}^{R} b_{kr} \phi_r(y) \qquad (3)$$

where $h = h(y)$. The structure functions are represented by ϕ_r, and their (complex) coefficients are given by b_{kr}. For a typical model domain, a set of R structure functions would be used to represent the boundary flows along each open boundary. Note that the expansion is expressed in terms of transport, since barotropic tidal velocities scale roughly with depth. The purpose of (3) is to allow the boundary flows to be parameterized by a smaller number of coefficients than the number of boundary grid points.

We have assumed that the tidal flows across the open boundaries are periodic in time, with known frequency. As the shallow water equations (1) define a damped linear system, the interior sea level and velocities are also assumed periodic in time with the same frequency

Table 1. Variance Partitioning for the Current Meters and ADCP

Current Meter	Depth,m	Tides	Wind	Residual	Total
c1	33	267	29	47	341
c2	20	232	24	81	335
c3	20	275	27	52	353
ADCP	-	183	14	116	342

The current meter (c1, c2, c3) and ADCP variance, in $cm^2\ s^{-2}$, is decomposed into tides (M_2, S_2, K_1, O_1), wind, and a residual. The current meter calculations are outlined in Section 2 and those for the ADCP in Section 5.

as the boundary forcing, but with a different amplitude and phase. This fact allows the shallow water equations to be recast in the frequency domain. Assuming that $\vec{u}, \eta$ have a time dependence of the form $e^{i\omega t}$, the shallow water equations (1) can be written

$$\begin{aligned}(i\omega + \lambda/h)\vec{u} + f\vec{k} \times \vec{u} + g\nabla\eta &= 0 \\ i\omega\eta + \nabla \cdot (\vec{u}h) &= 0 \qquad (4)\end{aligned}$$

where $\vec{u}, \eta$ are now redefined as the complex amplitudes of their respective variables. The solution to these equations is a boundary value problem which requires specification of the complex amplitudes of the boundary flows. This transformation of the shallow water equations into the frequency domain allows the explicit temporal dependence to be removed from the equations.

The discrete form of the boundary value problem (2)-(4), including the K tidal constituents of interest, can be represented by the matrix equation (see Appendix A)

$$\mathbf{u} = \mathbf{Db}. \qquad (5)$$

In this equation, $\mathbf{u}$ is a vector which represents the complex amplitudes of the interior tidal velocities $\vec{u}$ on the model grid for all the tidal constituents. The vector

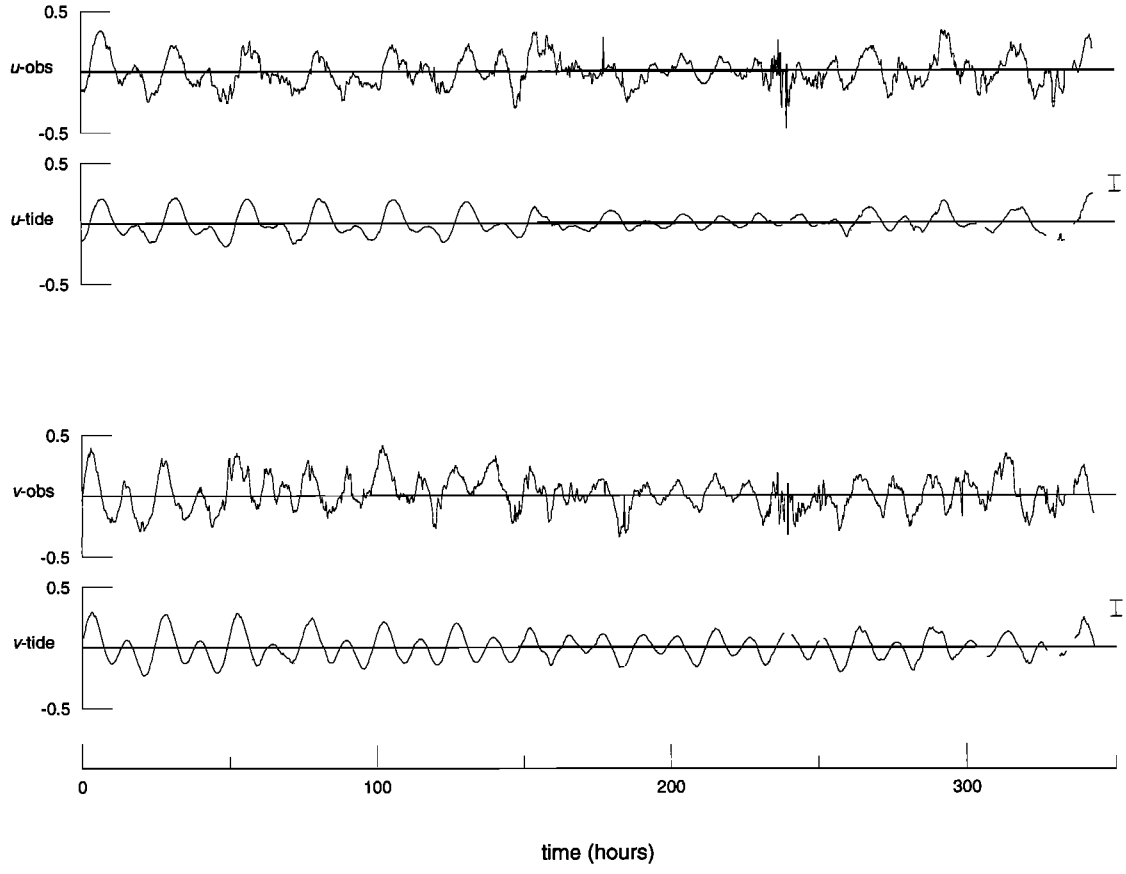

Figure 3. Time series plots of the observed ADCP data and estimated tidal components (in $m\,s^{-1}$) using M_2, S_2, K_1, O_1 (see section 5). The east-west component of the observed depth averaged current, and the estimated barotropic tide are denoted by u-obs and u-tide, respectively. (Similar notation is used for the north-south component v.) The plots also show a typical width for the 95% confidence interval. Gaps in the record indicate that the ship moved outside the model domain. The series begins at 2115, April 20, 1992.

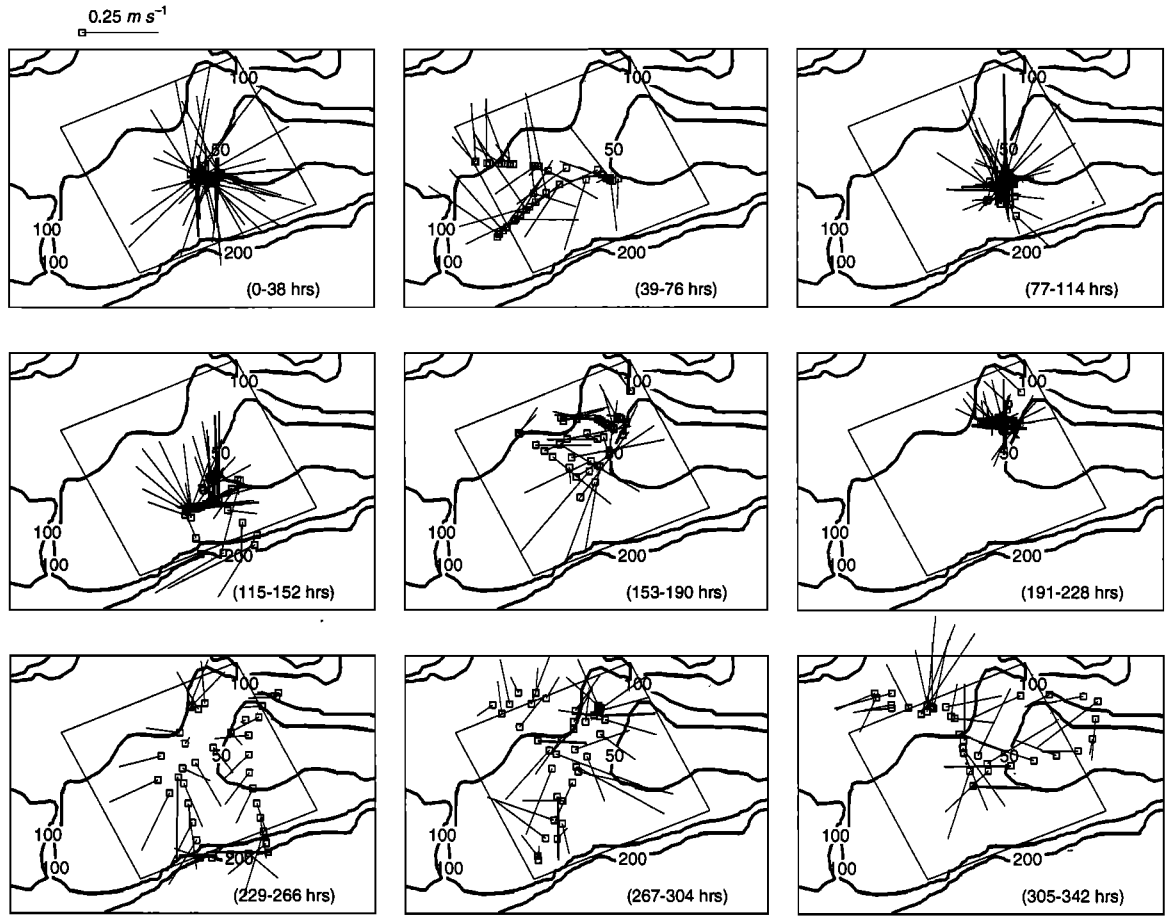

Figure 4. Vector plots of the observed depth averaged currents for the ADCP using a time interval of 1 hour beginning 2115, April 20, 1992. The contours represent the bathymetry of the region, and the large box is the study area (model domain). The small open squares represent the location of the ship, and the associated straight lines are the current vectors.

b contains the coefficients b_{kr} and describes the tidal flows across the open boundary. The dynamics matrix **D** contains a discrete analog to the shallow water equations (4) for each of the tidal frequencies and provides a mapping between the boundary and interior flows (Appendix A). Dimensions for these matrices are given in Table 2.

4. Inverse Analysis

The tidal extraction procedure presented here fits the shallow water equations to the time-space series of ADCP velocity using generalized least squares regression. The tidal model is treated as a strong constraint inasmuch as the velocity in the model interior is determined exactly by specifying the boundary state and solving the dynamic equations. As a result, the boundary conditions can be treated as the unknown quantities to be estimated from the ADCP record.

The first step in the tidal analysis requires a means of comparing the model predictions, given in the frequency domain, to ADCP data, obtained in the time domain. In the study of *McIntosh and Bennett* [1984], a frequency domain model, similar to (4), was used to analyze current and sea level time series from fixed moorings. These data were transformed into the frequency domain by a simple harmonic analysis, making the data directly comparable to the model variables. In contrast, *Lardner et al.* [1993] used a time stepping tidal model together with observed tidal time series from fixed locations. In the case of a ship-borne ADCP, the comparison of model to data is more complicated.

Consider a single observation z_t measuring one velocity component at a particular location at time t. The model counterpart $\hat{z}_t$ to the observation is

$$\hat{z}_t = \mathbf{s}_t' \sum_{k=1}^{K} \Re\{\mathbf{u}_k \, e^{i\omega_k t}\} \tag{6}$$

where the prime denotes transpose and $\mathbf{u}_k$ represents the complex amplitudes of the tidal velocity at the model grid points for the kth tidal constituent (Appendix A). The spatial interpolation vector $\mathbf{s}_t$ represents a linear operator which maps from the model grid to the observation location at time t. Note that, in general, this vector changes through time, reflecting the fact that measurement location is not fixed.

Table 2. Definition of Selected Matrices and Their Dimensions

Matrix	Size	Description
$\mathbf{u}$	$NK \times 1$	Complex amplitude of interior velocity at the model grid points including all K tidal constituents.
$\mathbf{b}$	$RK \times 1$	Coefficients of structure functions for the complex amplitude of velocity normal to the model boundary for the K tidal constituents.
$\mathbf{D}$	$NK \times RK$	Dynamics matrix mapping from $\mathbf{b}$ to $\mathbf{u}$ and derived from the shallow water equations in the frequency domain.
$\mathbf{u}_k$	$N \times 1$	Complex amplitude of interior velocity at the model grid points for the kth tidal constituent.
z_t	1×1	Observation of a single velocity component at time t.
$\mathbf{z}$	$L \times 1$	Vector containing observed horizontal velocity components over time.
$\mathbf{s}_t$	$N \times 1$	Spatial interpolator to map velocities on model grid at time t to a single measurement location.
$\mathbf{H}$	$L \times NK$	Overall interpolation matrix producing model counterparts to observations.

N is the total number of u and v points on the model grid, R is the number of spatial structure functions needed to describe the complex amplitudes of velocity points at the model boundaries for a single tidal constituent, K is the number of tidal constituents and L is the number of u and v observations.

Extending this to an observation vector $\mathbf{z}$ containing all the velocity components measured over time gives model counterparts $\hat{\mathbf{z}}$ to the observations

$$\hat{\mathbf{z}} = \Re\{\mathbf{Hu}\} \tag{7}$$

where $\mathbf{H}$ includes both the spatial and temporal interpolation implied by (6). This clarifies the process of comparing model output in the frequency domain with observations in the time domain when those observations include a spatial dimension.

The basis of the inverse analysis is the regression equation

$$\mathbf{z} = \hat{\mathbf{z}} + \mathbf{e}$$

where the error $\mathbf{e}$ is the tidal residual and measures the discrepancy between the observations and the model predictions. This error is of unknown character with its second-order properties described by the covariance matrix $\mathbf{V}$. Using (5) and (7), and converting all matrices and vectors to their real forms [e.g., *Brillinger* 1981, section 3.7], gives a regression equation of the form

$$\begin{aligned} \mathbf{z} &= \mathbf{Hu} + \mathbf{e} \\ &= \mathbf{HDb} + \mathbf{e}. \end{aligned} \tag{8}$$

The first equation of (8) contains no dynamics, and the problem of minimizing the error would involve estimating the interior tidal velocities $\mathbf{u}$ from the ADCP observations $\mathbf{z}$. Besides the problem of estimating a large number of unknowns from available observations, the dynamical links between the $\mathbf{u}$ are ignored and the resulting solution may have little physical meaning. The second equation of (8) includes shallow water dynamics which impose spatial structure on the interior and greatly reduces the number of unknowns by expressing the interior velocities in terms of the boundary flows.

Generalized least squares regression minimizes the weighted sum of squares of the error to yield an optimal estimate $\hat{\mathbf{b}}$ for the unknown boundary flows $\mathbf{b}$ in terms of the ADCP observations $\mathbf{z}$

$$\hat{\mathbf{b}} = (\mathbf{D'H'V^{-1}HD})^{-1}\mathbf{D'H'V^{-1}z}. \tag{9}$$

Estimates of the complex amplitude of the tidal velocities in the model interior $\hat{\mathbf{u}}$, the velocity along the ship track $\hat{\mathbf{z}}$, and associated error estimates are easily obtained (Appendix B).

To justify the strong constraint formalism used here, note that our inverse method may be viewed simply as an extension of traditional harmonic analysis techniques which fit sinusoids to time series data. As such, the analysis is not intended to explain the full variability of the observations, only that part specifically due to the barotropic tide. (From the current meter data in Table 1, we might expect the tides to explain at most 75% of the variance.) As a result, it is reasonable to assume that any model error term added to (5) is unnecessary, since the tidal residual $\mathbf{e}$ is expected to be of a much larger magnitude. This is, of course, provided that the model is an adequate one for the region, i.e., the assumptions of the tidal model (1) are satisfied.

Suppose that a weak constraint formalism was required. In this case, model errors would be added to (5), which would modify the error covariance structure in (8). That is, not only would the tidal residual need to be parameterized but so also would the dynamical errors in modeling the barotropic tide. Given the uncertainty in this, and the expected (small) magnitude of its effect, we have chosen to remain with the strong constraint method.

It is also straightforward to introduce into the analysis any additional regularization terms, such as smoothing operators. They enter as prior information, or "bogus" data [*Thacker*, 1988], on the boundary or interior flows. Mathematically, regularization adds another matrix (usually positive definite) to the bracketed term in (9), thereby better conditioning the inversion. This

technique closely resembles ridge regression in statistics, and the weight given the regularization term can be chosen through cross-validation techniques [*Golub et al.*, 1979].

To summarize, we have posed the tidal analysis of ADCP data as a highly overdetermined regression problem. Careful attention has been paid to reducing the number of parameters to be estimated by writing the interior flows in terms of suitably parameterized boundary flows. The spatial structure functions of (3) also ensure that the number of unknowns remains constant irrespective of grid resolution. As a result, the need for introducing additional regularization terms (e.g., spatial smoothing) is not anticipated.

5. Application

The tidal and subtidal variability of Western Bank circulation are now examined using the ADCP data described in section 2. Guided by the current meter results, the (separable) tidal constituents chosen for the analysis were M_2, S_2, K_1 and O_1. The domain of the limited area tidal model is shown in Figure 1. Its dimensions are approximately 120 km by 120 km, and it is oriented so as to be roughly parallel to the shelf break. The model has four open boundaries and uses an Arakawa C-grid. The interior dimensions of the grid include 14×14 η points, 14×13 u points, and 13×14 v points The open boundary is composed of 14 u points on the east and west boundaries and 14 v points on the north and south boundaries. The grid spacing was 8 km.

Note that although this application is realistic for the Western Bank case, it involves a relatively simple model having small dimensions. The method is, however, easily extended and computationally feasible for larger problems with complex geometry.

Consider the specification of the unknown boundary flows $\mathbf{b}$. Chebyshev Type II polynomials were chosen for the basis set ϕ_r. Numerical experiments indicated that only the first basis function ($r = 1$), the mean transport across each boundary, was required in this application. For our case, including higher order structure functions gave a marginally better fit to the ADCP data, but estimates in data-sparse regions were unrealistic, indicating model overfitting.

The frequency domain model given by (4) was finite differenced on the above grid and written directly as the required matrix equation (5). Given the grid described above and the four tidal constituents, the resulting matrix dimensions were the following: the state vector in the model interior $\mathbf{u}$ was 2912×1, the dynamics matrix $\mathbf{D}$ was 2912×32, the interpolation matrix $\mathbf{H}$ was 2744×2912, the data vector $\mathbf{z}$ was 2744×1, and the unknown boundary flow vector $\mathbf{b}$ was 32×1 (Table 2). Note that the quantity $\mathbf{HD}$ was evaluated directly using (6). The regression analysis of (9) thus involved inverting a 32×32 matrix.

Error estimates require that the covariance of the tidal residual $\mathbf{V}$ be specified. It was assumed that errors in the north-south v and east-west u components of the current are independent, allowing treatment of the two components of the tidal residual separately. (In fact, their *a posteriori* correlation coefficient was 0.16.) The tidal residuals for both u and v were found to be serially correlated following a first-order autoregressive (AR(1)) process. The estimated autoregressive coefficients imply a decorrelation time of about 1.5 hours for the residuals. Given this AR(1) error structure, the error covariance matrix $\mathbf{V}$ and its inverse are easily determined [*Morrison*, 1967, section 8.11]).

Tidal ellipses for M_2, S_2, K_1, and O_1 estimated by this analysis are shown in Figure 5. These estimates were found to be stable over a wide range of grid resolutions, values for the friction coefficients and errors in the bathymetry. The ellipses scale roughly with depth, being generally larger in the shallow water and smaller in the deep water. The M_2 tide dominates the region and, along with the two diurnal constituents, accounts for most of the variation in the tidal signal. Overall, the ellipse maps agree with previous calculations for the Scotian Shelf region [*Gregory*, 1988]. Table 1 indicates that the tides account for about 60% of the variance in the ADCP record. This is a lower proportion than for the current meters, suggesting that the ADCP record is influenced by additional nontidal processes which are, at least, partly due to the ship's movement.

To further test the ADCP tidal estimates, the results were also compared to ellipses derived from the three current meters deployed near the center of the model domain. Figure 6 shows this comparison and indicates that the current meter ellipses match well those derived from the ADCP and, in all but one case (c3, S_2), fall within the estimated 95% confidence regions. For the relatively weak flows associated with S_2 and O_1, Figure 6 also suggests that the estimated ellipses are not significantly different from zero. To further refine the estimates, additional ADCP data sets widely separated in time could easily be used in the analysis of section 4. Furthermore, the current meter data itself can be included in the inverse calculation but, in this case, it has been withheld for model validation purposes.

The estimated tidal currents along the cruise track of the ship $\hat{\mathbf{z}}$ are shown in Figure 3. This estimated tidal time series shows the spring-neap cycle and semidiurnal and diurnal oscillations. These periodic oscillations exhibit small discrete jumps over the length of the record which become more pronounced toward the end. These are a result of the changes in depth along the ship track which the model grid further accentuates when interpolating to the observation locations. The approximate width of the 95% confidence intervals is 0.07 ms^{-1}. However, it does vary slightly over the length of the record, depending on the measurement location, ranging from 0.06 ms^{-1} to 0.09 ms^{-1}.

The estimated error in the overall tidal flow field generally falls within this same range. Its magnitude depends on the duration of the ADCP record together with the (tidal) signal to noise ratio. The spatial variability of the error closely reflects the data distribution;

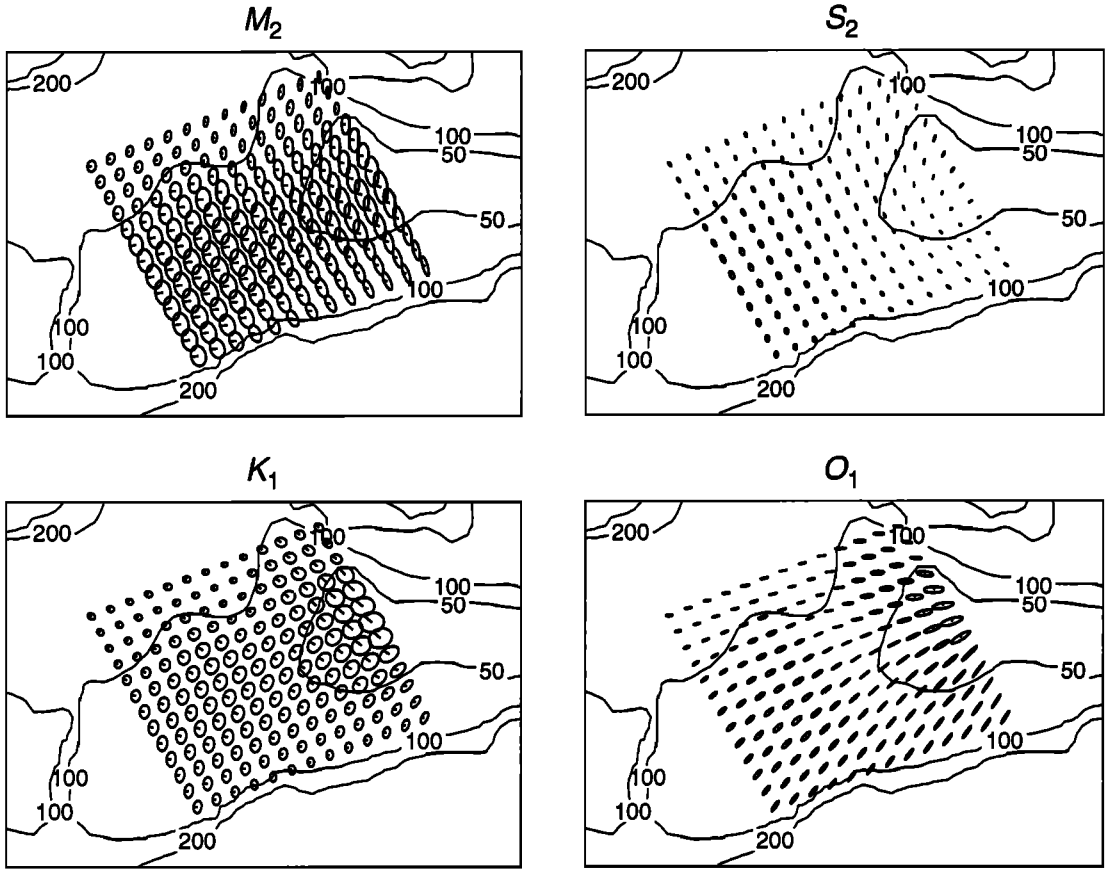

Figure 5. Tidal ellipse maps for M_2, S_2, K_1, O_1 estimated from the ADCP data and plotted at the model grid points. The ellipses are scaled to represent half the tidal excursion of the M_2 tide. The initial phase is represented by the straight line beginning at the center of each ellipse.

it is lower in the central region and higher in the data-sparse areas near the model boundary. The error field is also nearly identical for each of the four tidal constituents. Standard error ellipses are oriented mainly in the southwest-northeast direction. The major axes of the tidal ellipses often fall approximately perpendicular to this direction, implying that the overall amplitude of the tidal constituent is well captured, while its orientation is subject to some uncertainty.

Figure 7 shows vector plots of the tidal residual series. These are more easily interpreted than their counterparts in Figure 4, which include the tides. The residual currents are generally weaker, particularly in the central region near the crest of Western Bank. There is a suggestion of a persistent northward current in the western part of the region. However, this is difficult to see due to the irregular cruise track of the ship and presence of a wind-driven component to the circulation.

To remove the wind effect, the simple wind-driven model of section 2 was fit (using the same lagged values of the wind) to the ADCP tidal residual series. In this case, the wind model explains only about 10% of the variability in the de-tided ADCP record, in contrast to the nearly 30% explained for the de-tided current meter records. Again, the transfer function between the wind and ADCP record has a broad peak centered near the inertial frequency, but the corresponding direction of the flow is inconsistent with a simple Ekman flux to the right of the wind. Information on the wind-driven circulation appears to be buried in the multitude of other signals recorded by the ADCP as the ship moves throughout the region.

To isolate the steady part of circulation, the ADCP residual (tides and wind removed) were binned into 0.2° latitude/longitude blocks. The result of this is shown in Figure 8 together with surface currents obtained from a diagnostic calculation (method of J. Sheng and K.R. Thompson, A robust method for diagnosing regional shelf circulation from observed density profiles, submitted to *Journal of Geophysical Research*, 1995; hereinafter referred to as submitted manuscript) using density data from 177 CTD casts obtained during the cruise (Figure 1). The general flow patterns obtained from the two sources are similar, both show an anticyclonic gyre centered on the crest of Western Bank and a persistent northward flow to the west of this gyre. This existence of this gyre has been confirmed with drifter deployments made during the cruise [*Sanderson*, 1995]. Note that a corresponding binning of the original ADCP data shows a series of almost randomly oriented vectors, indicating that the tides could not simply be averaged to obtain the residual.

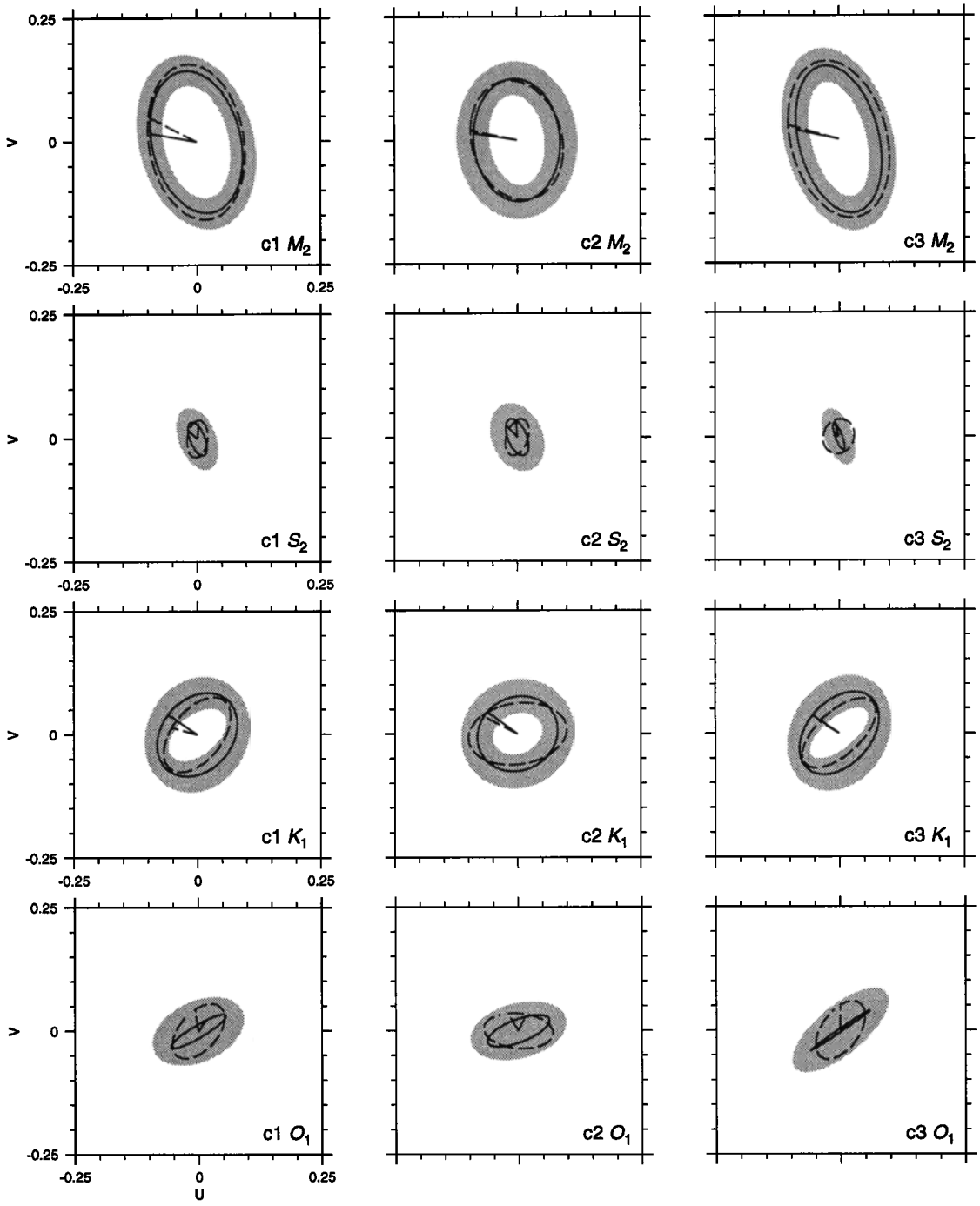

Figure 6. Comparison of M_2, S_2, K_1, O_1 tidal ellipses obtained from current meters c1, c2, and c3 (dashed lines) and those estimated from the ADCP at corresponding locations (solid lines). The initial phase is represented by the straight line beginning at the center of each ellipse. The shaded area represents the 95% confidence region for the estimated ADCP tidal ellipses; u and v denote the respective east-west and north-south components of current velocity in m s^{-1}.

6. Summary and Discussion

We have presented a conceptually straightforward method for de-tiding the velocity series obtained from a ship-borne ADCP. The method fits a limited area tidal model, based on shallow water dynamics, to the ADCP observations of depth-averaged velocity. More generally, the method provides a means to carry out harmonic analysis on a time-space series of velocity. We offer this as an alternative to the procedure of *Candela et al.* [1992] where arbitrary spatial interpolation functions were fitted to the ADCP velocities. Our proposed method does, however, require additional effort beyond that *Candela et al.* [1992] since a tidal model is implemented as part of the analysis procedure.

Application of the method to estimating tidal flows from ship ADCP data from the Western Bank region

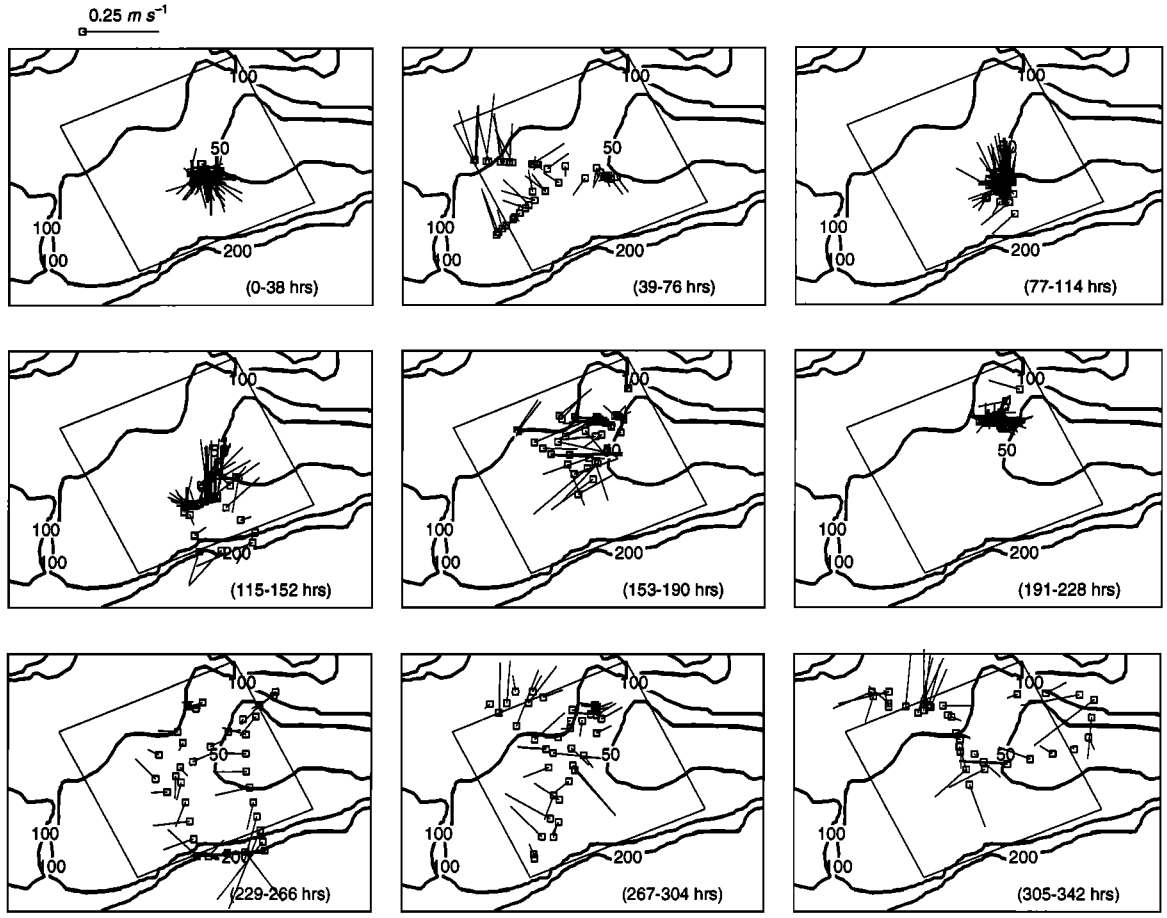

Figure 7. Vector plots of the estimated tidal residuals for the hourly ADCP data beginning 2115, April 20, 1992. Contours represent the bathymetry of the region and the large box is the study area (model domain). The small open squares represent the location of the ship, and the associated straight lines are the current vectors.

of the Scotian Shelf appears successful. The estimated tidal ellipses obtained from the ADCP record match those obtained from current meter records and regional tidal maps. The weaker tidal constituents are less consistent with these independent sources but within estimated error limits. The residual field, after removal of the tides and the wind-driven circulation, clearly showed a gyre centered on Western Bank and a persistent northward flow to its west. These features are also confirmed using other data sources obtained on the April 1992 cruise.

Some additional considerations arise in the tidal extraction from a time-space series. One concern is the ability of the analysis to separate closely spaced frequency bands when a spatial dimension is included in the series. Another concern is that the tides may be aliased by the movement of the ship. To test for this possibility in the Western Bank case, a simulated velocity time series was generated by sampling the flow field of the diagnostic calculation in Figure 8 along the cruise track of the ship. Performing the tidal analysis on this series showed no evidence of existence of any spurious tidal signals.

The use of generalized least squares regression has a correspondence with other commonly used assimilation techniques. The general problem solved here is one of minimizing the weighted squared observation/model discrepancy

$$J = (\mathbf{z} - \hat{\mathbf{z}})' \mathbf{V}^{-1} (\mathbf{z} - \hat{\mathbf{z}}). \tag{10}$$

The model counterparts to the data $\hat{\mathbf{z}}$ are constrained to satisfy the shallow water equations (1). The condition making this applicable to tidal flows is that the normal flows across the open boundary are further constrained to be periodic in time with known frequency but an unknown complex amplitude $\mathbf{b}$. In this paper, the estimate $\hat{\mathbf{b}}$ which minimizes J is found by transforming the shallow water equations into the frequency domain and expressing them as a discrete boundary value problem in matrix form. The model counterparts to the data are then written in terms of the unknown $\mathbf{b}$. Differentiation of J with respect to the unknown $\mathbf{b}$ and setting the result equal to zero yields an estimate for the boundary state $\hat{\mathbf{b}}$.

Consider another case in which it is desired to use a time stepping numerical tidal model [e.g. *Lardner*, 1993]. To minimize J subject to such a model posed in the time domain, optimal control/adjoint approaches can prove useful. The minimum of J with respect to $\mathbf{b}$ can be found iteratively using a Lagrange multiplier

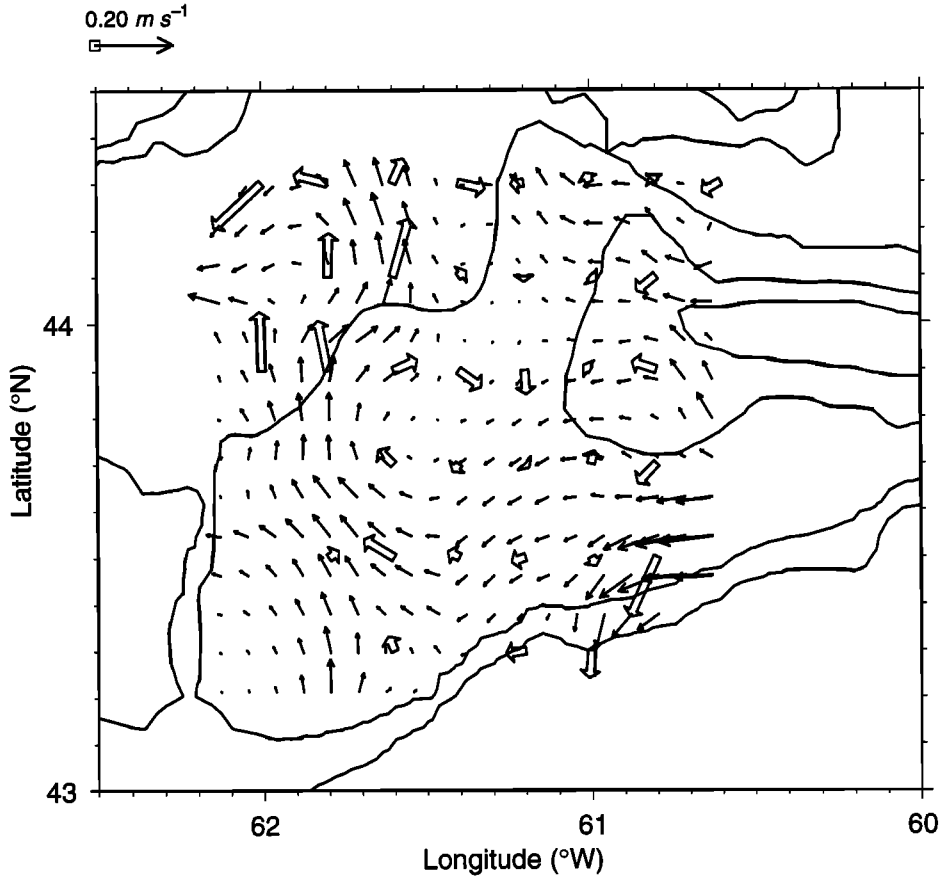

Figure 8. Comparison of the residual circulation on Western Bank derived from the ADCP (open arrows) and a diagnostic calculation of the flow field (solid arrows). The ADCP residual is prepared by binning the residual (tide and wind effects removed) into 0.2° latitude/longitude boxes. The diagnostic calculation (method of J. Sheng and K.R. Thompson, submitted manuscript, 1995) estimates the surface circulation using 177 density profiles collected during the April 1992 cruise (Figure 1).

technique. Each iteration involves a cycle composing a forward integration of the model equations, a backward integration of the adjoint equations, and calculation of the gradient of J with respect to the unknown quantities. The gradient information is used along with a descent algorithm to converge on the minimum [e.g., *Thacker and Long*, 1988]. For the present problem this approach was extremely inefficient, as illustrated below.

The above variational procedure was applied to the tidal analysis of the ADCP data using a fully explicit finite difference form of the shallow water equations (1) on the identical model grid used for the frequency domain model. The time step, set by the CFL condition, was 120 s. A forward integration of this model required about 5 model days to reach a periodic steady state and a further 14 model days to produce model counterparts to the data. The adjoint equations required a similar amount of computation time. A minimum of 20 iterations were required to achieve convergence, and the final estimates were essentially equal to those found by the statistical-dynamical approach of this paper. Error analysis of the estimates would involve computing the second derivatives of J with respect to $\mathbf{b}$, i.e., the Hessian matrix. In addition to the large computational cost compared to the approach of this paper, numerical experimentation also pointed to additional concerns related to proper radiation of wave energy in such a boundary control problem.

Other solution techniques may be necessary if the dynamic assumptions implied by the linearized, depth averaged shallow water equations are not met. One possibility is to retain the linear model and introduce model errors explicitly into the analysis (section 4). Another approach is to use a more complicated model. For instance, to analyze the internal tides in the deep water regions surrounding Western Bank from the current profiles would require at least a two-layer model. A time stepping model, with model errors, can be approached using Kalman smoother [*Bryson and Ho*, 1969; chaps. 12 and 13] or representer solutions [*Bennett* 1992, section 5.4]. Finally, inclusion of nonlinear advective terms would transform the problem into one of nonlinear regression and suggest the use of more general variational data assimilation techniques.

In summary, we have presented, and applied, a method for extracting the barotropic tide from a ship-borne ADCP record. The procedure fits a tidal model to ADCP data using generalized least squares regression with the primary advantage that the shallow water dynamics provide spatial interpolation functions. Realis-

tic error estimates are produced as an intermediate step in the calculation. The procedure relies solely on ADCP data and can utilize records separated widely in time. In addition, for the application in this paper, no arbitrary regularization terms, such as spatial smoothness, were required to get well-conditioned solutions. Overall, the method should allow an ADCP tidal residual to be obtained efficiently and be minimally contaminated by the de-tiding procedure.

Appendix A: The Dynamics Matrix

Tidal dynamics are governed by the shallow water equations posed in the frequency domain, i.e., the boundary value problem of (2)-(4). For the kth tidal constituent, this problem can be expressed in discrete form as

$$\mathbf{D}_k^{\text{LHS}} \begin{pmatrix} \mathbf{u}_k \\ \eta_k \end{pmatrix} = \mathbf{D}_k^{\text{RHS}}\, \mathbf{b}_k.$$

The vector $\mathbf{b}_k$ contains the coefficients b_{kr} of (3) which describe the tidal flows across the open boundary. The vectors $\mathbf{u}_k$ and η_k contain the complex amplitudes of the velocity and sea level defined on the interior model grid points. The matrices $\mathbf{D}_k^{\text{LHS}}$ and $\mathbf{D}_k^{\text{RHS}}$ are derived by finite differencing the shallow water dynamics (4).

Premultiplying both sides by the inverse of $\mathbf{D}_k^{\text{LHS}}$ and retaining only the rows of $(\mathbf{D}_k^{\text{LHS}})^{-1}\mathbf{D}_k^{\text{RHS}}$ corresponding to the $\mathbf{u}_k$ yields

$$\mathbf{u}_k = \mathbf{D}_k \mathbf{b}_k.$$

The matrix $\mathbf{D}_k$ has complex entries and represents a mapping of the model boundary conditions to the interior flow for a single tidal constituent.

To include the full set of K tidal constituents introduce the following:

$$\begin{pmatrix} \mathbf{u}_1 \\ \vdots \\ \mathbf{u}_K \end{pmatrix} = \begin{pmatrix} \mathbf{D}_1 & \cdots & \mathbf{0} \\ \vdots & \ddots & \vdots \\ \mathbf{0} & \cdots & \mathbf{D}_K \end{pmatrix} \begin{pmatrix} \mathbf{b}_1 \\ \vdots \\ \mathbf{b}_K \end{pmatrix}$$

where the left-hand side contains the complex amplitudes of the tidal velocities at the model grid points. The right-hand side is composed of a block diagonal matrix, the blocks being the dynamics matrix for each of the different tidal frequencies. This matrix multiplies the set of complex amplitudes of the boundary flows parameterized in terms of spatial structure functions. The above equation may be expressed more concisely as

$$\mathbf{u} = \mathbf{D}\mathbf{b}$$

which represents the complete tidal system in the frequency domain corresponding to (4) and the boundary conditions (2) and (3). The dimensions of these quantities in relation to the model grid and number of tidal constituents is summarized in Table 2.

Note that the dynamics matrix $\mathbf{D}$ can be obtained in at least two different ways. One method involves finite differencing the shallow water equations in the frequency domain (4) and writing the equations directly into matrix form given above. Alternatively, if a suitable time stepping numerical tidal model based on (1) exists for the region, $\mathbf{D}$ may be generated as follows. Impose periodic flows across a portion of the open boundaries corresponding to one element of $\mathbf{b}$ and, furthermore, use radiation conditions on the remaining open boundaries. Integrate the model to a periodic steady state and perform a harmonic analysis of the interior velocities to yield the response $\mathbf{u}$ to a single element of $\mathbf{b}$ and therefore a column of the matrix $\mathbf{D}$. By continuing this process with respect to each element of $\mathbf{b}$, the full matrix $\mathbf{D}$ can be sequentially obtained.

Appendix B: Regression Analysis

The ADCP data $\mathbf{z}$ can be expressed in terms of the boundary flows $\mathbf{b}$ through the regression equation (8)

$$\mathbf{z} = \mathbf{H}\mathbf{D}\mathbf{b} + \mathbf{e}$$

where the error $\mathbf{e}$ represents the tidal residual whose second order properties are described by the covariance matrix $\mathbf{V}$.

Generalized least squares regression minimizes the weighted sum of squares of the error $J = \mathbf{e}'\mathbf{V}^{-1}\mathbf{e}$ to yield an estimate for $\mathbf{b}$ in terms of the data $\mathbf{z}$. Differentiating J with respect to $\mathbf{b}$ and setting the result to zero yields

$$\hat{\mathbf{b}} = (\mathbf{D}'\mathbf{H}'\mathbf{V}^{-1}\mathbf{H}\mathbf{D})^{-1}\mathbf{D}'\mathbf{H}'\mathbf{V}^{-1}\mathbf{z}$$

where $\hat{\mathbf{b}}$ is the estimate for $\mathbf{b}$ which minimizes J (the maximum likelihood estimate under the assumption of a normally distributed $\mathbf{e}$). An estimate of the interior field $\hat{\mathbf{u}}$ is then obtained using (5) as

$$\hat{\mathbf{u}} = \mathbf{D}\hat{\mathbf{b}}$$

and the estimate for the model counterparts to the data is

$$\hat{\mathbf{z}} = \mathbf{H}\mathbf{D}\hat{\mathbf{b}}.$$

Error estimates are also easily obtained as a part of the regression calculation. The covariances of $\hat{\mathbf{b}}$, $\hat{\mathbf{u}}$, and $\hat{\mathbf{z}}$ are [e.g., *Sen and Srivastiva* 1990, chap. 2]

$$\begin{aligned} \text{cov}(\hat{\mathbf{b}}) &= (\mathbf{D}'\mathbf{H}'\mathbf{V}^{-1}\mathbf{H}\mathbf{D})^{-1} \\ \text{cov}(\hat{\mathbf{u}}) &= \mathbf{D}(\mathbf{D}'\mathbf{H}'\mathbf{V}^{-1}\mathbf{H}\mathbf{D})^{-1}\mathbf{D}' \\ \text{cov}(\hat{\mathbf{z}}) &= \mathbf{H}\mathbf{D}(\mathbf{D}'\mathbf{H}'\mathbf{V}^{-1}\mathbf{H}\mathbf{D})^{-1}\mathbf{D}'\mathbf{H}'. \end{aligned}$$

These quantities are used to determine confidence intervals for the estimates $\hat{\mathbf{b}}$, $\hat{\mathbf{u}}$, and $\hat{\mathbf{z}}$.

Acknowledgments. This research was funded through the Ocean Production Enhancement Network (OPEN), under the Canadian Centres of Excellence program. We are grateful to Dr. David Griffin for a great deal of help, including the preparation of the ADCP and other cruise data. Dr. Jinyu Sheng provided continued support including the

diagnostic calculation of the mean circulation on Western Bank shown in Figure 8. We also thank Dr. W.C. Thacker for making clear the connection between the "adjoint" approach to data assimilation and the procedure used in this paper.

References

Bennett, A.F., *Inverse Methods in Physical Oceanography*, 346 pp., Cambridge Univ. Press, New York, 1992.

Bennett, A.F., and P.C. McIntosh, Open ocean modeling as an inverse problem: Tidal theory, *J. Phys. Oceanogr., 12*, 1004-1018, 1982.

Brillinger, D.R., *Time Series. Data Analysis and Theory*, 540 pp., Holden-Day, Merrifield, Va., 1981.

Bryson, A.E., and Y. Ho, *Applied Optimal Control*, 481 pp., Blaisdell, Waltham, Mass., 1969.

Candela, J., R.C. Beardsley, and R. Limeburner, Separation of tidal and subtidal currents in ship mounted acoustic Doppler current profiler observations, *J. Geophys. Res., 97*, 769-788, 1992

Das, S.K., and R.W. Lardner, On the estimation of parameters of hydraulic models by assimilation of periodic tidal data, *J. Geophys. Res., 96*, 15,187-15,196, 1991.

Foreman, M.G.G., and H.J. Freeland, A comparison of techniques for tide removal from ship mounted acoustic Doppler measurements along the southwest coast of Vancouver Island, *J. Geophys. Res., 96*, 17,007-17,021, 1991.

Geyer, W.R., and R. Signell, Measurements of tidal flow around a headland with a shipboard acoustic Doppler current profiler, *J. Geophys. Res., 95*, 3189-3197, 1990.

Godin, G., *The Analysis of Tides*, 264 pp., Univ. of Liverpool Press, London, 1972.

Golub, G., M. Heath, and G. Wahba, Generalized cross validation as a method for choosing a good ridge parameter, *Technometrics, 21*, 215-223, 1979.

Gregory, D.N., Tidal current variability on the Scotian shelf and slope, *Can. Tech. Rep. Hydrogr. Ocean Sci., 109*, 1988.

Griffin, D. and S. Lochmann, Petrel V cruise 22 to Western Bank, *OPEN Report 1992/6*, Dep of Oceanogr., Dalhousie Univ., Halifax, Nova Scotia, Canada, 1992.

Howarth, M.J., and R. Proctor, Ship ADCP measurements and tidal models of the North Sea, *Continental Shelf Res., 12*,. 601-623, 1992.

Lardner, R.W., Optimal control of open boundary conditions for a numerical tidal model, *Computer Methods in Applied Mechanics and Engineering, 102*, 367-387, 1993.

Lardner, R.W., A.H. Al-Rabeh, and N. Gunay, Optimal estimation of parameters for a two-dimensional hydrodynamical model of the Arabian Gulf, *J. Geophys. Res., 98*, 18,229-18,242, 1993.

Marmorino, G.O. and C.L. Trump, Acoustic Doppler current profiler measurements of possible lee waves south of Key West, Florida, *J. Geophys. Res., 97*, 7271-7275, 1992.

McIntosh, P.C., and A.F. Bennett, Open ocean modeling as an inverse problem, M2 tides in the Bass Strait, *J. Phys. Oceanogr., 14*, 601-614, 1984.

Morrison, D.F., *Multivariate Statistical Methods*, 338 pp., McGraw-Hill, New York, 1967.

Pollard, R.T., and R.C. Millard, Comparison between observed and simulated wind-generated inertial oscillations, *Deep Sea Res., 17*, 813-821, 1970.

Sanderson, B.G., Structure of an eddy measured with drifters. *J. Geophys. Res., 100*, 6761-6776, 1995.

Sen, A., and M. Srivastava, *Regression Analysis: Theory, Methods, and Applications*, 347 pp., Springer-Verlag, New York, 1990.

Simpson, J.H., E.G. Mitchelson-Jacob and A.E. Hill, Flow structure in a channel from an acoustic Doppler current profiler. *Continental Shelf Res., 10*, 589-603, 1990.

Smith, P.C., and F.B. Schwing, Mean circulation and variability on the eastern Canadian continental shelf, *Continental Shelf Res., 11*, 977-1012, 1991.

Thacker, W.C., Fitting models to inadequate data by enforcing spatial and temporal smoothness, *J. Geophys. Res., 93*, 10,655-10,665, 1988.

Thacker, W.C., and R.B. Long., Fitting dynamics to data, *J. Geophys. Res., 93*, 1227-1240, 1988.

M. Dowd and K.R. Thompson, Department of Oceanography, Dalhousie University, Halifax, Nova Scotia, Canada, B3H 4J1.

(Received September 7, 1994; revised April 25, 1995; accepted July 20, 1995.)